Photonic Crystals & MEMS

- Fundamentals of Photonic-Crystal Sensors
  - High reflectivity, broad band reflectors
- Fiber Microphones/Hydrophones
- Photon-tunneling Position Sensors
  - Mode coupling controlled by symmetry
- Fabrication - GOPHER
  - Compatible with MEMS, CMOS, and SMF
- Conclusions

Onur KILIÇ 2006

PC Applications

Microresonators (LDs and LEDs)

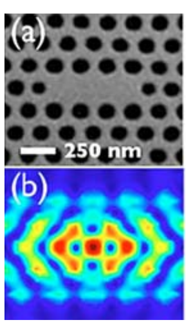

Optical tuning of PCs
Fushman, Vučković et al, APL 90, 091118, 07

Waveguides and Integrated Optics

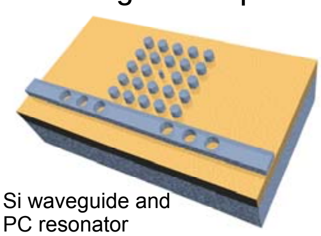

Si waveguide and PC resonator

Waveguide resonator coupled to high-Q, PC resonator. The coupling is tuned through the free-carrier effect

Holey Fiber

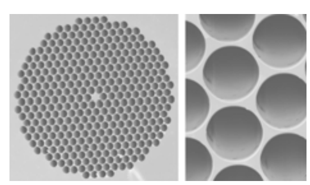

SEM of a PC fiber (US Naval Research Laboratory). The diameter of the solid core is 5 μm, while the diameter of the holes is 4 μm (Wikipedia)

© os, 2/12/2008

PC Mirrors, Filters, and Sensors

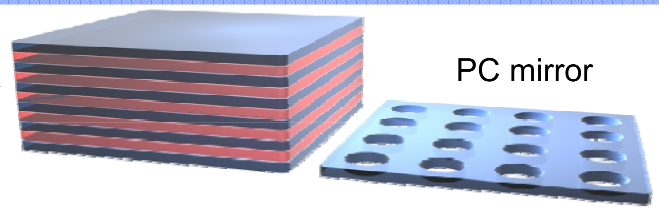

- Mirrors:
  - Broad operating bandwidth, Low polarization dependence, and Large angular range compared to DBRs
  - Higher reflectivity and more robust than metals
- Sensors/Filters:
  - Lithographic control of spectral features – flexible multiplexing
  - Photon tunneling sensors by symmetry breaking
- Polarization control:
  - Birefringence controlled by lithography
- Fabrication:
  - Single dielectric layer, compact, MEMS compatible, flexible (different substrates)

© os, 2/12/2008

O.Solgaard
Stanford

Photonic Crystal Mirrors, Filters and Sensors

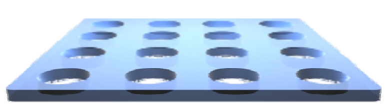

Photonic Crystal Slab (PCS)

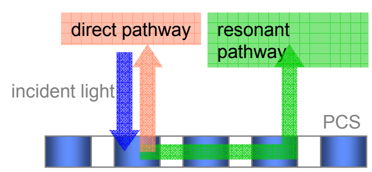

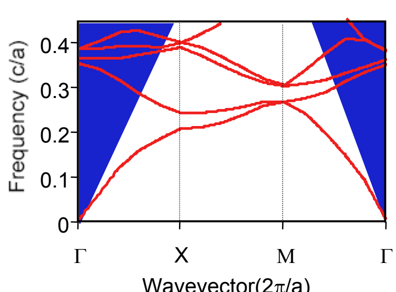

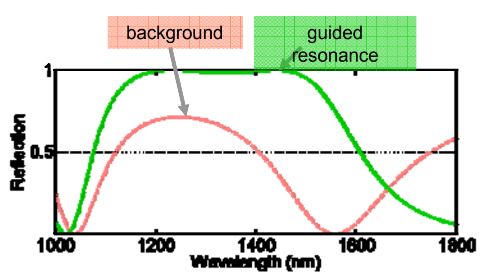

© os, 2/12/2008

O.Solgaard
Stanford

Applications

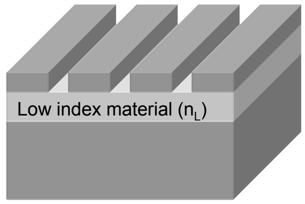

C.F.R. Mateus, C. Chang-Hasnain,et. al., July 2004

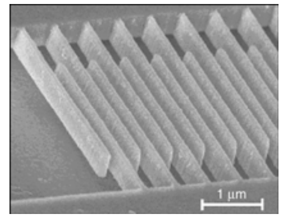

D.W. Carr, Sandia, OL vol. 28, 18, Sept. 15, 2003

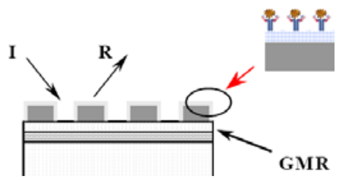

R. Magnusson, U. Connecticut, LEOS 07, TuJ1

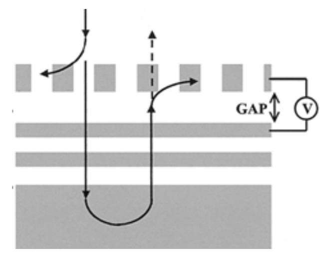

Viktorovitch, JLT, vol. 21, 7, July 2003

© os, 2/12/2008

Photonic Crystal Acoustic Sensor

- A compact, fiber-based microphone with no electrical parts
- Intended for underwater acoustic detection (hydrophone)
- High sensitivity at high acoustic frequencies
  - Acoustic wave moves diaphragm
  - Photonic crystal mirror and fiber-end mirror forms a F-P interferometer
  - Reflected power changes with a change in the diaphragm-fiber gap

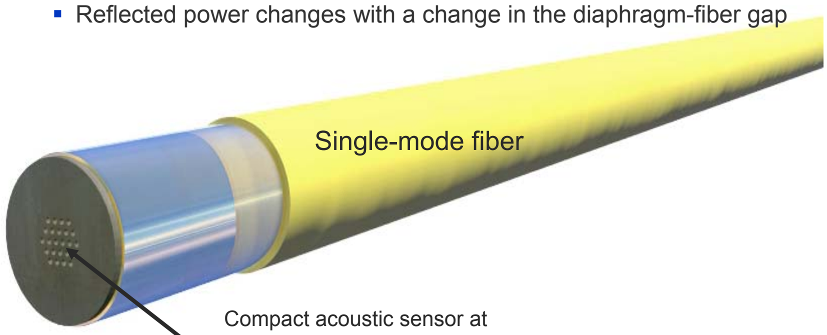

Compact acoustic sensor at the end of a single-mode fiber

© os, 2/12/2008

How does the acoustic sensor work?

- Acoustic wave moves diaphragm (150 - 300 µm diameter)
- Photonic-crystal mirror and fiber-end mirror forms a Fabry-Perot interferometer
- Reflected power in fiber changes with a change in the diaphragm-fiber gap
  - Photonic-crystal mirror provides a very thin, high reflectivity mirror, so that the Fabry-Perot is low order and has a high finesse (15 - 30)
  - 4-orders-of-magnitude better detection limit than similar types of diaphragm-fiber sensors

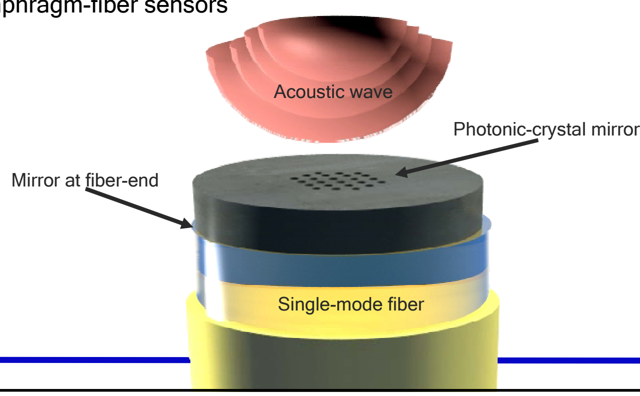

1st Order F-P

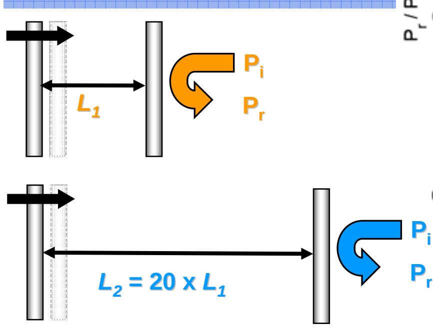

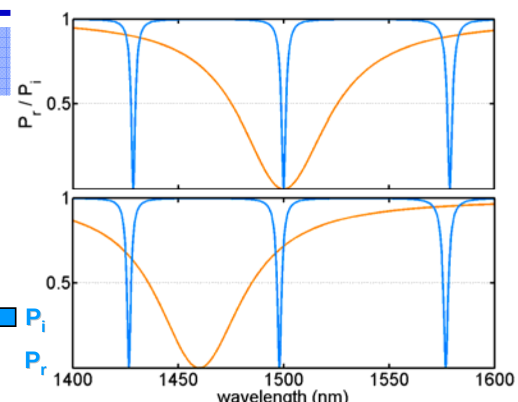

- For the same displacement of the mirror: $\Delta Power_{long} = \Delta Power_{short}$
- For the same temperature variation: $\Delta Power_{long} = 20 \times \Delta Power_{short}$

Conclusion:
- Same sensitivity for any cavity length, but short cavity has:
  - Better temperature stability
  - Broader resonance, hence no laser stability problems
  - Mechanical robustness

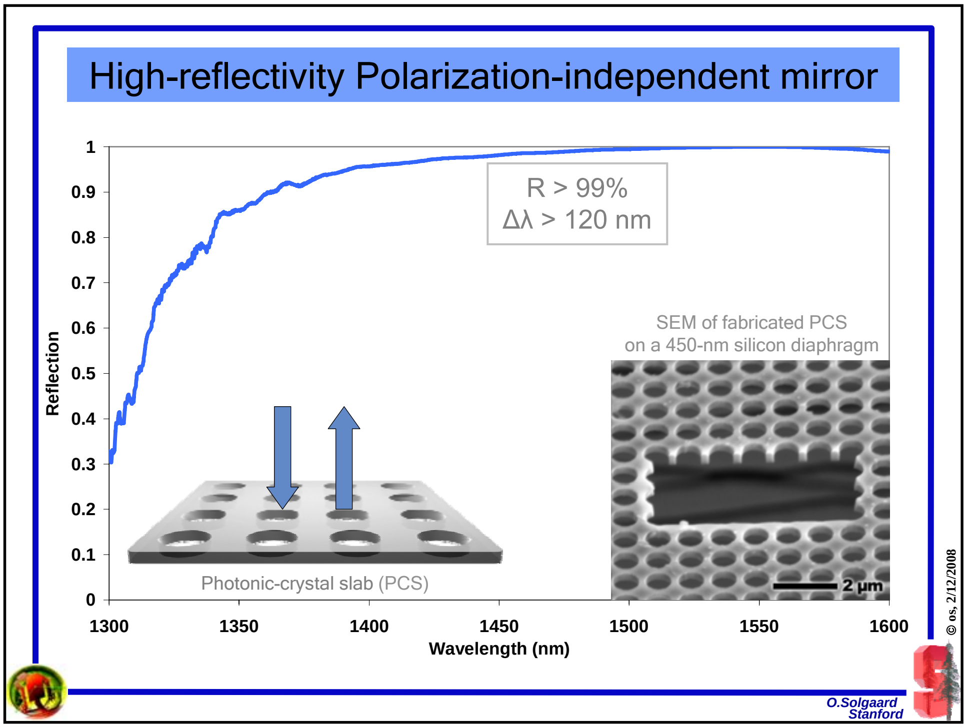
High-reflectivity Polarization-independent mirror
R > 99%
Δλ > 120 nm
SEM of fabricated PCS
on a 450-nm silicon diaphragm
Photonic-crystal slab (PCS)
2 μm
Reflection
0
0.1
0.2
0.3
0.4
0.5
0.6
0.7
0.8
0.9
1
1300
1350
1400
1450
1500
1550
1600
Wavelength (nm)
© os, 2/12/2008
O.Solgaard
Stanford

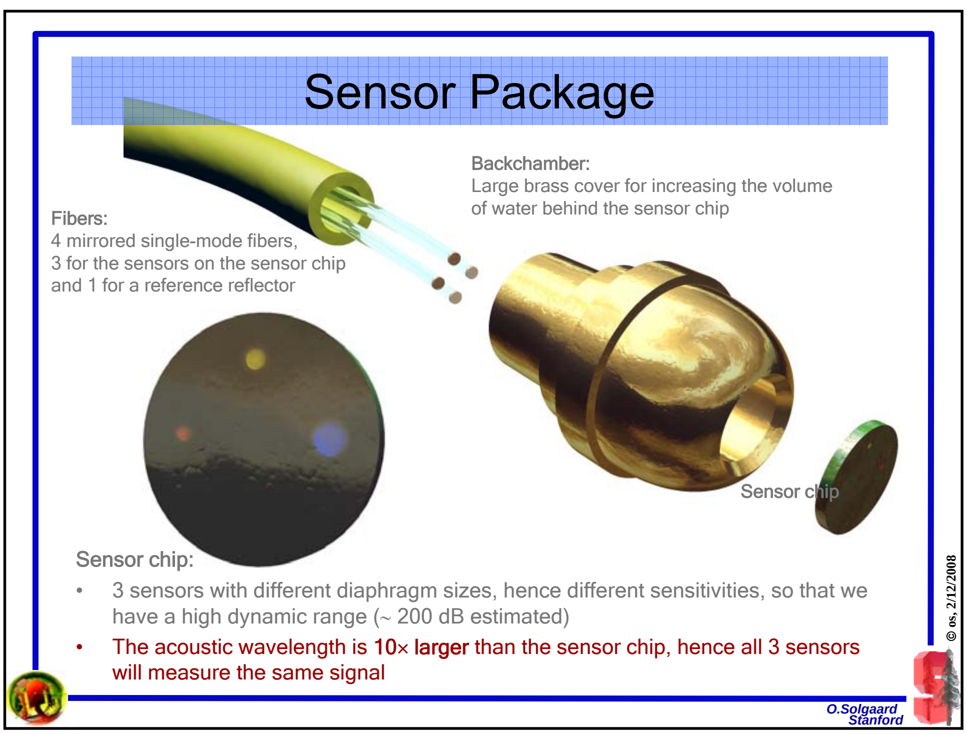
Sensor Package
Backchamber:
Large brass cover for increasing the volume
of water behind the sensor chip
Fibers:
4 mirrored single-mode fibers,
3 for the sensors on the sensor chip
and 1 for a reference reflector
Sensor chip
Sensor chip:
• 3 sensors with different diaphragm sizes, hence different sensitivities, so that we have a high dynamic range (~ 200 dB estimated)
• The acoustic wavelength is 10× larger than the sensor chip, hence all 3 sensors will measure the same signal
© os, 2/12/2008
O.Solgaard
Stanford

Power response at 30 KHz

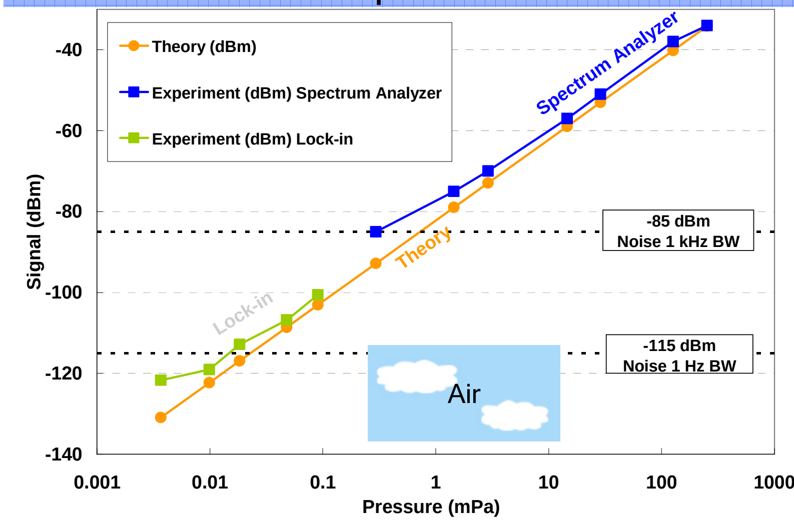

- Detected a minimum pressure of 18 μPa in a 1-Hz bandwidth
- Corresponds to a minimum detectable displacement of $1\text{x}10^{-14}$ m
- Detected an **estimated** 100 μPa in a 1-Hz bandwidth **in water**

O.Solgaard
Stanford

© os, 2/12/2008

Hydrophone in nature

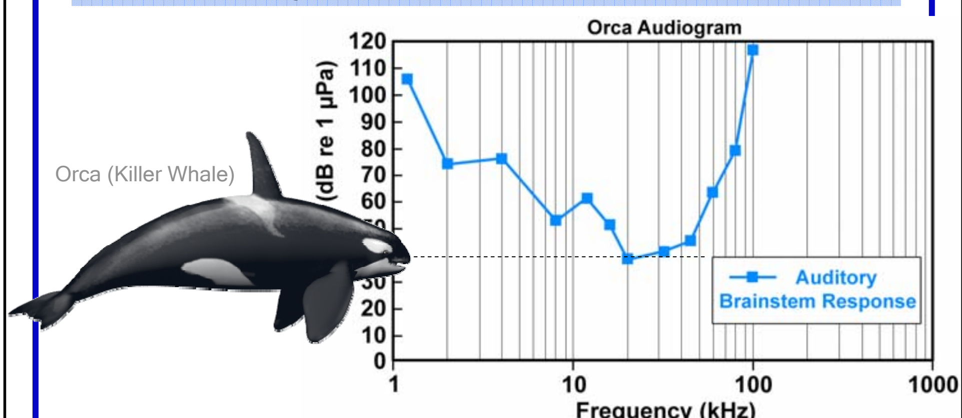

- Uses both passive and active listening
- Can locate big/small and slow/fast objects
- Echolocation: navigation and terrain mapping

Audiogram from Szymanski *et al.* J. Acoust. Soc. Am. **106**, 1134-1141 (1999)

O.Solgaard
Stanford

© os, 2/12/2008

Summary

- Demonstrated compact, packaged, fiber-based acoustic sensor based on photonic-crystal slabs (PCS), with no electrical parts, intended for underwater acoustic detection
  - PCS provides high reflectivity, optically thin, mechanically compliant mirror with venting holes
  - Characterized microphone with a minimum detectable pressure (MDP) of 18 μPa/Hz$^{1/2}$ in air (10^{-4} Å displacement), with a relatively flat frequency response up to > 50 kHz
  - Characterized hydrophone with estimated MDP of ~ 100 μPa/Hz$^{1/2}$
  - We expect to reach a MDP of 1.6 μPa/Hz$^{1/2}$ in air and 12 μPa/Hz$^{1/2}$ in water, **down to the ambient noise level**

Packaged fiber-based acoustic sensor

Near Field Coupling – Lateral Shift

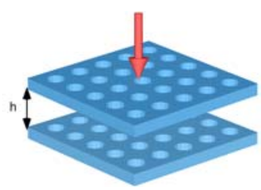

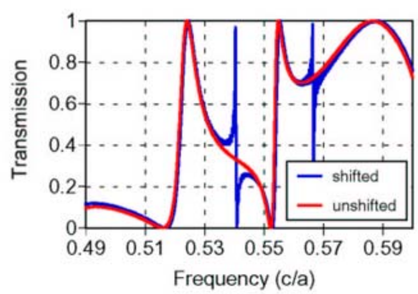

- Transmission spectra through two coupled PCs
- The crystal structure consists of a square lattice of air holes of radius 0.4*a*, where *a* is the lattice constant, introduced into a dielectric slab. The slab has a dielectric constant of 12 and a thickness of 0.55*a.* The spacing between the slabs is 0.1a.
- The red curve corresponds to a structure with holes in two slabs aligned to each other vertically
- The blue curve corresponds to a structure with the lattice of holes in the top slab shifted by a distance of 0.05a along the (10) direction with respect to the bottom slab

© os, 2/12/2008

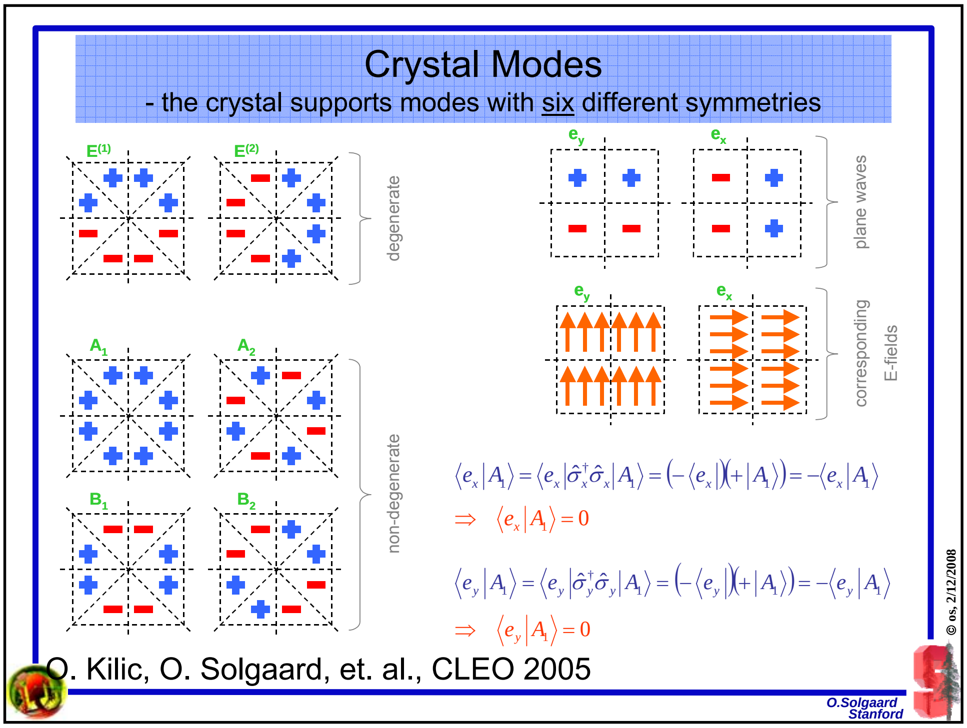
Crystal Modes
- the crystal supports modes with six different symmetries
E(1)
E(2)
degenerate
A1
A2
B1
B2
non-degenerate
ey
ex
plane waves
corresponding E-fields
$\langle e_x|A_1\rangle = \langle e_x|\hat{\sigma}_x^\dagger\hat{\sigma}_x|A_1\rangle = (-\langle e_x|)(+|A_1\rangle) = -\langle e_x|A_1\rangle$
$\Rightarrow \langle e_x|A_1\rangle = 0$
$\langle e_y|A_1\rangle = \langle e_y|\hat{\sigma}_y^\dagger\hat{\sigma}_y|A_1\rangle = (-\langle e_y|)(+|A_1\rangle) = -\langle e_y|A_1\rangle$
$\Rightarrow \langle e_y|A_1\rangle = 0$
O. Kilic, O. Solgaard, et. al., CLEO 2005
O.Solgaard
Stanford
© os, 2/12/2008

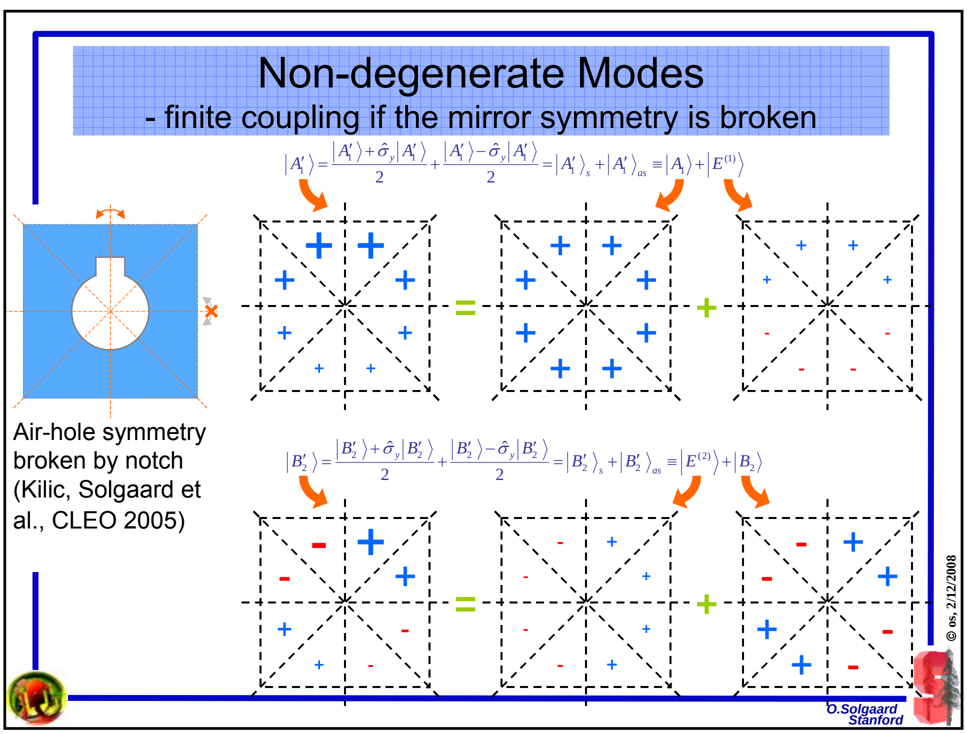
Non-degenerate Modes
- finite coupling if the mirror symmetry is broken
$|A_1'\rangle = \frac{|A_1'\rangle + \hat{\sigma}_y|A_1'\rangle}{2} + \frac{|A_1'\rangle - \hat{\sigma}_y|A_1'\rangle}{2} = |A_1'\rangle_s + |A_1'\rangle_{as} \equiv |A_1\rangle + |E^{(1)}\rangle$
Air-hole symmetry broken by notch (Kilic, Solgaard et al., CLEO 2005)
$|B_2'\rangle = \frac{|B_2'\rangle + \hat{\sigma}_y|B_2'\rangle}{2} + \frac{|B_2'\rangle - \hat{\sigma}_y|B_2'\rangle}{2} = |B_2'\rangle_s + |B_2'\rangle_{as} \equiv |E^{(2)}\rangle + |B_2\rangle$
O.Solgaard
Stanford
© os, 2/12/2008

PC Displacement Sensor
- principle of operation

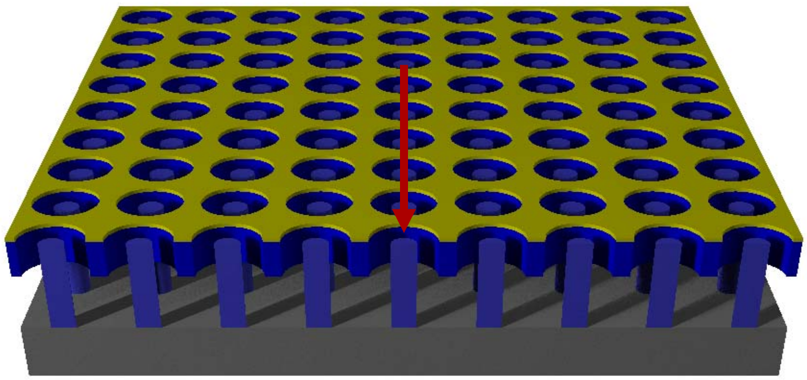

© os, 2/12/2008

O.Solgaard
Stanford

PC Displacement Sensor
- principle of operation

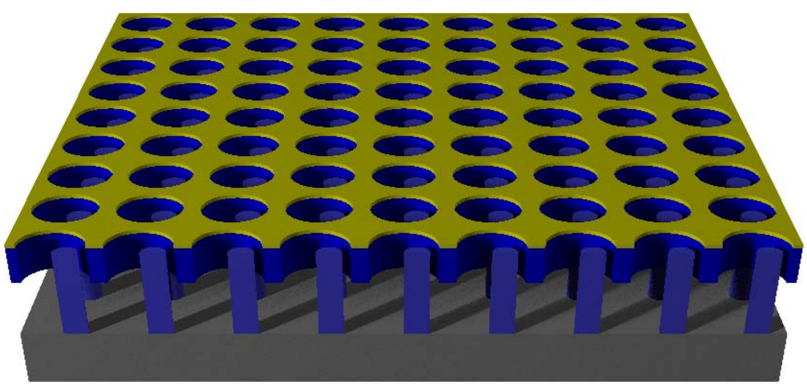

© os, 2/12/2008

O.Solgaard
Stanford

Tunable PC Fabrication

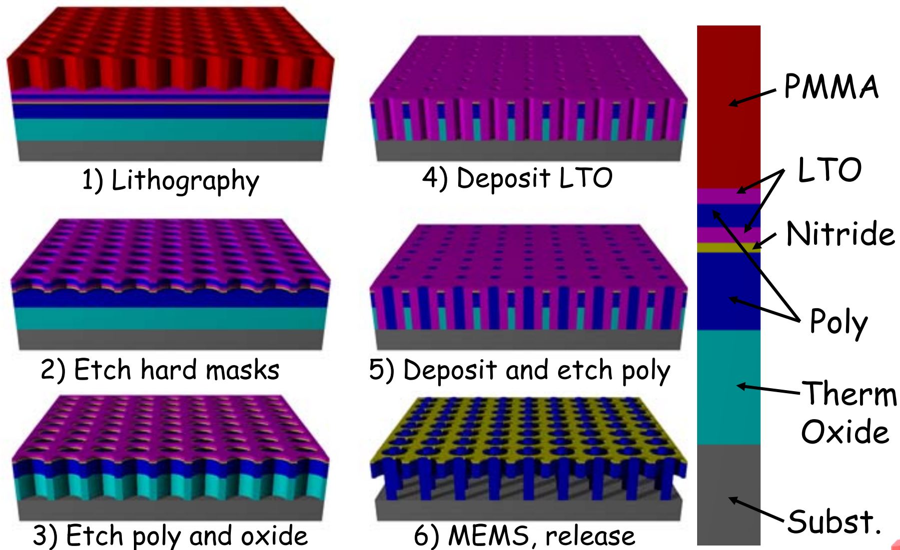

© os, 2/12/2008

2-D PC Fabrication

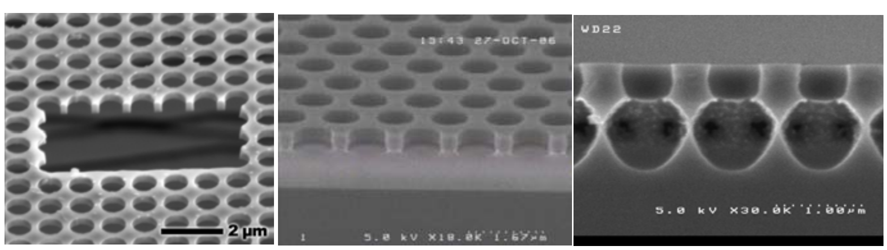

450-nm SOI diaphragm | Polysilicon on Silicon Oxide | PC etched into Si substrate

- Typical dimensions:
  - Pitch: 1um, hole diameter: 700 nm, membrane thickness: 450 nm
- Lithography:
  - E-beam, nano-imprint, optical, FIB

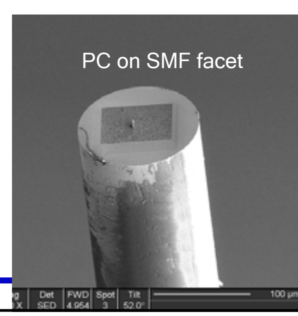

© os, 2/12/2008

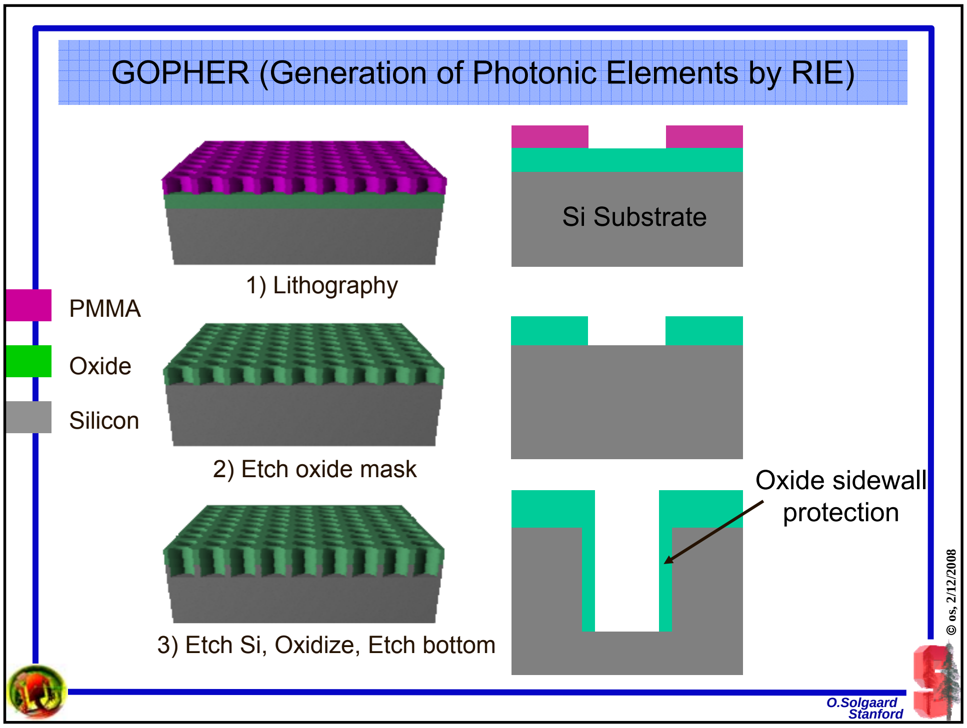
GOPHER (Generation of Photonic Elements by RIE)
Si Substrate
1) Lithography
PMMA
Oxide
Silicon
2) Etch oxide mask
Oxide sidewall protection
3) Etch Si, Oxidize, Etch bottom
© os, 2/12/2008
O.Solgaard Stanford

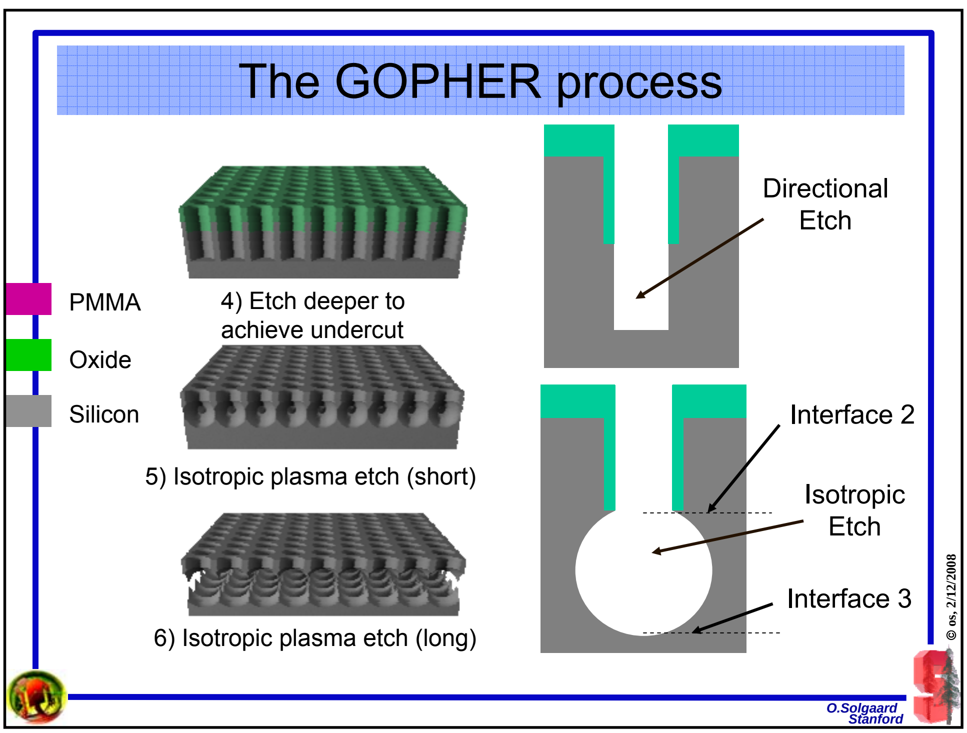
The GOPHER process
Directional Etch
PMMA
Oxide
Silicon
4) Etch deeper to achieve undercut
5) Isotropic plasma etch (short)
6) Isotropic plasma etch (long)
Interface 2
Isotropic Etch
Interface 3
© os, 2/12/2008
O.Solgaard Stanford

3-D GOPHER

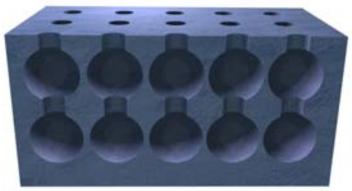

Multiple Layer Structures

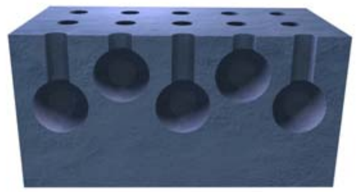

Vertically Offset Structures

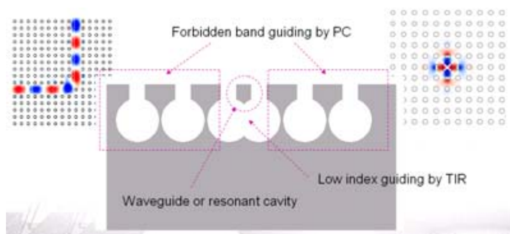

Waveguides/Resonators

© os, 2/12/2008

O.Solgaard
Stanford

2-D GOPHER

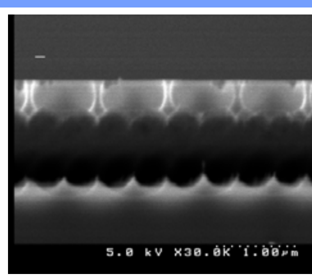

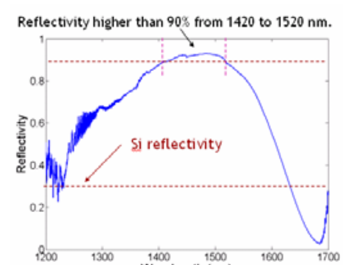

Completely released PC shows reflectivity >90% from 1420 to 1520 nm

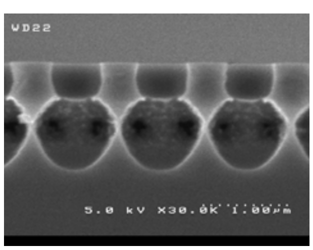

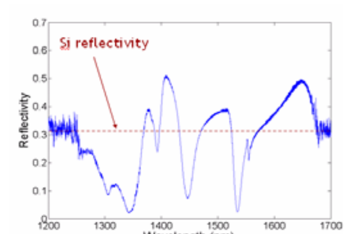

Partially undercut PC shows sharp resonance minimum around 1550 nm

© os, 2/12/2008

O.Solgaard
Stanford

Double Layer Gopher Structures

Reflectivity higher than 90% from 1575 to 1650 nm with the peak reaching 96%

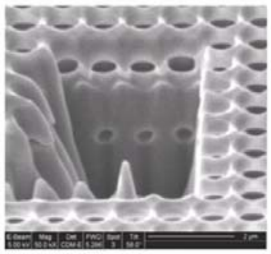

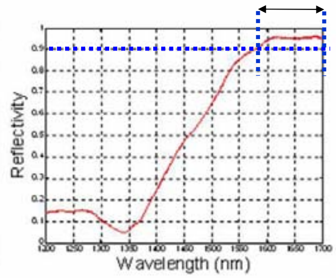

Very high reflectivity structure can be designed using two or more layers

S. Basu Mallick, S. Kim, S. Hadzialic, A. Sudbo, and O. Solgaard, "Double-layered Monolithic Silicon Photonic Crystals", submitted to CLEO 2008

© os, 2/12/2008

Restructuring through Hydrogen Annealing

Isotropically etched interface with sharp edges

Silicon surface smooth everywhere except at edges of protective oxide

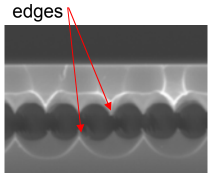

PC Cross Section before Hydrogen Anneal

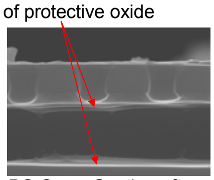

PC Cross Section after Hydrogen Anneal

At elevated temps. in Hydrogen, Si migrate to minimize surface energy, resulting in rounding of edges in silicon structures

Sora Kim, Rishi Kant, Sanja Hadzialic, Roger T. Howe, and Olav Solgaard, "Interface Quality Control of Monolithic Photonic Crystals by Hydrogen Annealing", submitted to CLEO 2008

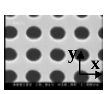

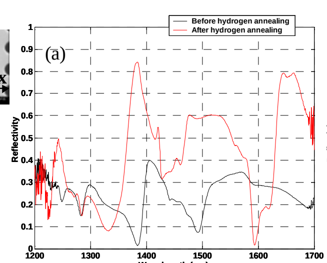

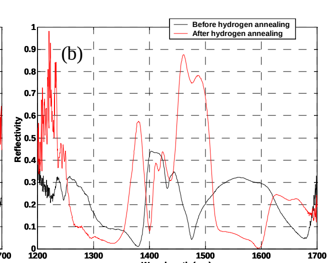

Measured reflection spectra for x (a) and y (b) polarizations

© os, 2/12/2008

Restructuring through H-Anneal

Smoother interface with rounded edges and more uniform and symmetric holes

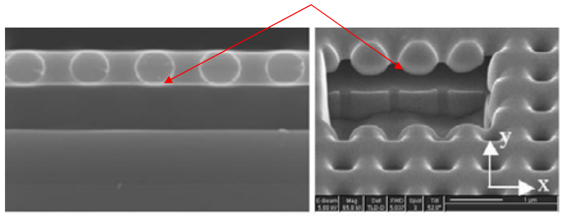

SEM of PCs following removal of sidewall oxide and subsequent hydrogen anneal

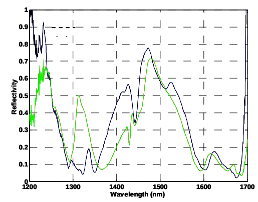

Reflection spectra for x (green) and y (black) polarizations

- Dependent on temperature, pressure, and annealing time
- Improves both surface roughness and structural uniformity
- Leads to improved optical performance

© os, 2/12/2008

Monolithic Si PC's

- Self-aligned structures fabricated by GOPHER
  - Interfaces created by alternate thermal oxidation and etch
  - High quality first reflection interface
  - Polished SCS surface with sub-nm RMS roughness and low stress
  - Compatible with high temperature and wet etch processing
  - IC compatible processing
  - 2-D and 3-D structures

High optical quality photonic crystal surface

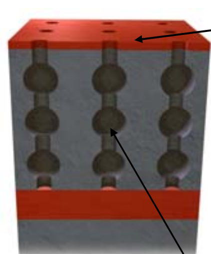

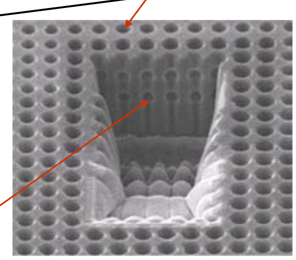

Two-layer PC with the center FIBed to show 3D structure

High index contrast interface created by an isotropic undercut

© os, 2/12/2008

Conclusions

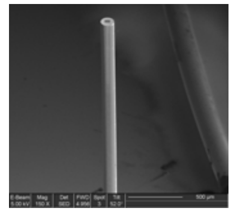

- Compact fiber microphones
  - Demonstrated MDP of 18 μPa/Hz$^{0.5}$ at frequencies up to 50 kHz
- High-sensitivity PC Displacement sensors based on symmetry breaking
  - Up to 58% modulation for 0 – 10 V actuation
  - Different mode symmetries allows displacement along two orthogonal direction to be distinguished
  - Applications: Pressure sensors, force sensors, inertial sensors, optical modulation

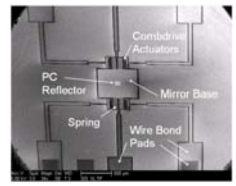

- GOPHER creates PC in monolithic SI
  - No internal stress, compatible with CMOS, resistant to high temperatures and wet etches
  - 2-D and 3-D PCs
  - Hydrogen Annealing to smoothen interfaces
  - Integration with MEMS/NEMS (PC scanner, Fiber Tip sensors)

© os, 2/12/2008

Acknowledgements

- Students:
  - Onur Can Akkaya, Christophe Antoine, Russ Belikov, Sanja Hadzialic, Il-Woong Jung, Rishi Kant, Onur Kilic, Sora Kim, Daesung Lee, Shrestha Basu Mallick, Hye-Jun Ra
- Postdocs
  - Il-Woong Jung, Wibool Piyawattanametha
- Research Scientists
  - Michael Mandela
- Faculty Collaborators:
  - Adela Ben-Yakar, Chris Contag, Michel Digonnet, Shanhui Fan, Roger Howe, Gordon Kino
- Research Support: Agilent, Boeing, Litton, DARPA, CIS, NIH

© os, 2/12/2008